

# Combined Synthetic, Spectroscopic, and Computational Insights Into a General Method for Photosensitized Alkene Aziridination

Alana Rose Meyer, Mihai V. Popescu, Arindam Sau, Niels H. Damrauer,\* Robert S. Paton,\* and Tehshik P. Yoon\*



Cite This: *ACS Catal.* 2024, 14, 12310–12317



Read Online

ACCESS |

Metrics & More

Article Recommendations

Supporting Information

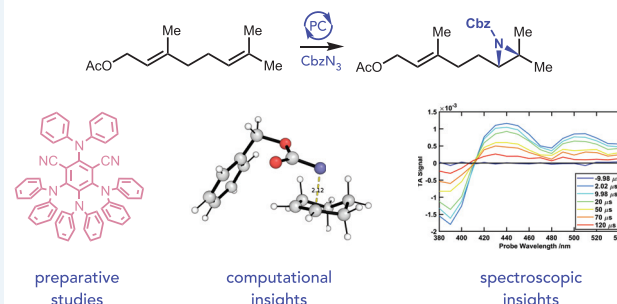
**ABSTRACT:** Aziridines are important targets for synthetic chemistry, and many methods involving the aziridination of alkenes by olefins with nitrenes have been reported. In general, however, nitrene transfer reactions are optimized for a limited range of nitrene precursors, and the synthesis of structurally diverse aziridines featuring a range of *N*-substituents requires the application of multiple methods with varying reaction conditions. Herein, we report a photocatalytic method for the aziridination of olefins that operates with a wide range of *N*-substituted nitrene precursors. A combination of synthetic, spectroscopic, and computational data is consistent with a mechanism involving the photocatalytic generation of triplet nitrene intermediates. The effectiveness of 4DPAIPN as a photocatalyst for this process can be rationalized as a consequence of its exceptionally long lifetime, rather than of its excited state energies or redox properties in isolation.

**KEYWORDS:** aziridination, triplet nitrene, photocatalysis, triplet energy transfer, photocatalytic mechanisms

## INTRODUCTION

The synthesis of aziridines remains an important problem in contemporary organic chemistry.<sup>1,2</sup> Many methods for the preparation of complex nitrogen-containing structures take advantage of the ring strain inherent in these small-ring heterocycles. Aziridines also serve as the reactive moieties in the mitomycins, azinomycins, and other DNA-modifying bioactive compounds.<sup>3,4</sup> As such, aziridines are useful for applications in synthesis and medicinal chemistry, although their value depends upon the availability of facile methods to prepare them with a high degree of structural diversity. Photocatalytic methods offer an attractive strategy for aziridine synthesis because of the ease by which nitrenes, nitrene radical ions, and other hypervalent nitrogen species are generated through photochemical activation.<sup>5,6</sup> Several years ago, we reported an Ir(III)-catalyzed method for photochemical aziridine synthesis that involves the triplet sensitization of Troc azide (Figure 1A).<sup>7</sup> This method provides selective access to the triplet state of the nitrene intermediate and high chemoselectivity for aziridine formation; it thus improves upon classical methods involving direct photoexcitation of azidoformates, which produce mixtures of singlet and triplet nitrenes and correspondingly afford allylic amination products in addition to the aziridination product.<sup>8,9</sup> Recently, Koenigs reported an alternate method for photoredox aziridination in which single-electron photoreduction of sulfonyliminiodinane

### photocatalytic aziridination using diverse nitrene precursors



was proposed to afford a nitrene radical anion intermediate.<sup>10–12</sup> Finally, during the preparation of this manuscript, Bouwman and Codée reported that the organic carbazole-based photocatalyst 4CzPN is effective triplet photosensitizer for aziridinations using sulfonyl azides as a nitrene precursor.<sup>13</sup>

Notably, each of these photocatalytic methods for the aziridination of alkenes is reported for a single nitrene precursor; the *N*-Troc and *N*-sulfonyl aziridines resulting from these methods are readily deprotected, but the strongly reducing conditions required are incompatible with many sensitive organic functional groups found in complex organic molecules. Indeed, few methods for alkene aziridination are tolerant of a wide range of *N*-substituents, and even well-developed transition-metal-catalyzed approaches are generally optimized to function with a single nitrene precursor.<sup>2,14</sup> We imagined that a more general method for aziridine synthesis would tolerate a wider range of nitrene precursors under a single set of conditions, enabling the direct installation of varied *N*-substituents that would be either of direct utility in

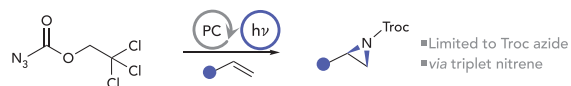
Received: May 29, 2024

Revised: July 17, 2024

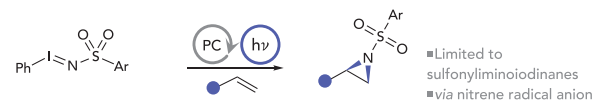
Accepted: July 19, 2024

## A. Visible light induced aziridination methods

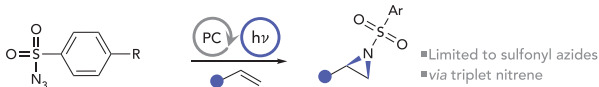
Yoon and coworkers (2017)



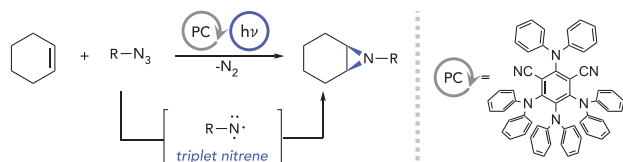
Koenigs and coworkers (2022)



Codeé and coworkers (2024)



## B. Aziridination enabled by general nitrene formation strategy (this work)



advantage: compatible with carbamate, acyl, and sulfone azides

**Figure 1.** (A) Recent developments in photocatalytic olefin aziridination. (B) General photosensitized olefin aziridination enabled by an organic photosensitizer.

synthetic applications or cleaved using one of several common, mild, and orthogonal deprotection conditions (Figure 1B).

The goals of the studies described in this paper are two-fold. First, we hoped to develop an improved photocatalytic system that enables a broader range of organic azides to be activated and utilized in synthetically useful aziridination reactions. Second, because the photochemical activation of azides could potentially result in the generation of multiple reactive intermediates (e.g., triplet nitrenes, singlet nitrenes, nitrene radical ions, or aminyl radicals), we imagined that a combination of experimental and computational techniques could better elucidate the mechanism of this reaction and provide a roadmap for rational development of other photocatalytic amination reactions. Herein, we describe the

results of this investigation, which resulted in a significantly more general method for photocatalytic aziridination, and we employ a variety of techniques that collectively demonstrate that this reaction likely proceeds through the intermediacy of a photogenerated triplet nitrene.

## METHODS AND MATERIALS

In our previous study, optimized conditions utilized  $[\text{Ir}(\text{ppy})_2(\text{dtbbpy})]\text{PF}_6$  (3a) as the photosensitizer, and Troc azide proved to be a uniquely reactive nitrene precursor for aziridination reactions; simpler alkyl carbamoyl azides lacking electron-withdrawing halogen substituents are not efficiently sensitized and provide much lower yields of aziridines. We surmised that this sensitivity would prevent the simple photocatalytic system we previously reported to be used for the synthesis of aziridines featuring *N*-Boc, *N*-Cbz, *N*-Fmoc, or other more common protecting groups. In line with this expectation, irradiation of Cbz azide (1), cyclohexene, and Ir photocatalyst 3a with a 427 nm Kessil lamp gave modest yield of aziridine 2 (Table 1; entry 1). Consistent with the results of our previous optimization studies, a screen of other Ir-based photocatalysts did not improve the yield (Table 1; entries 2 and 3).

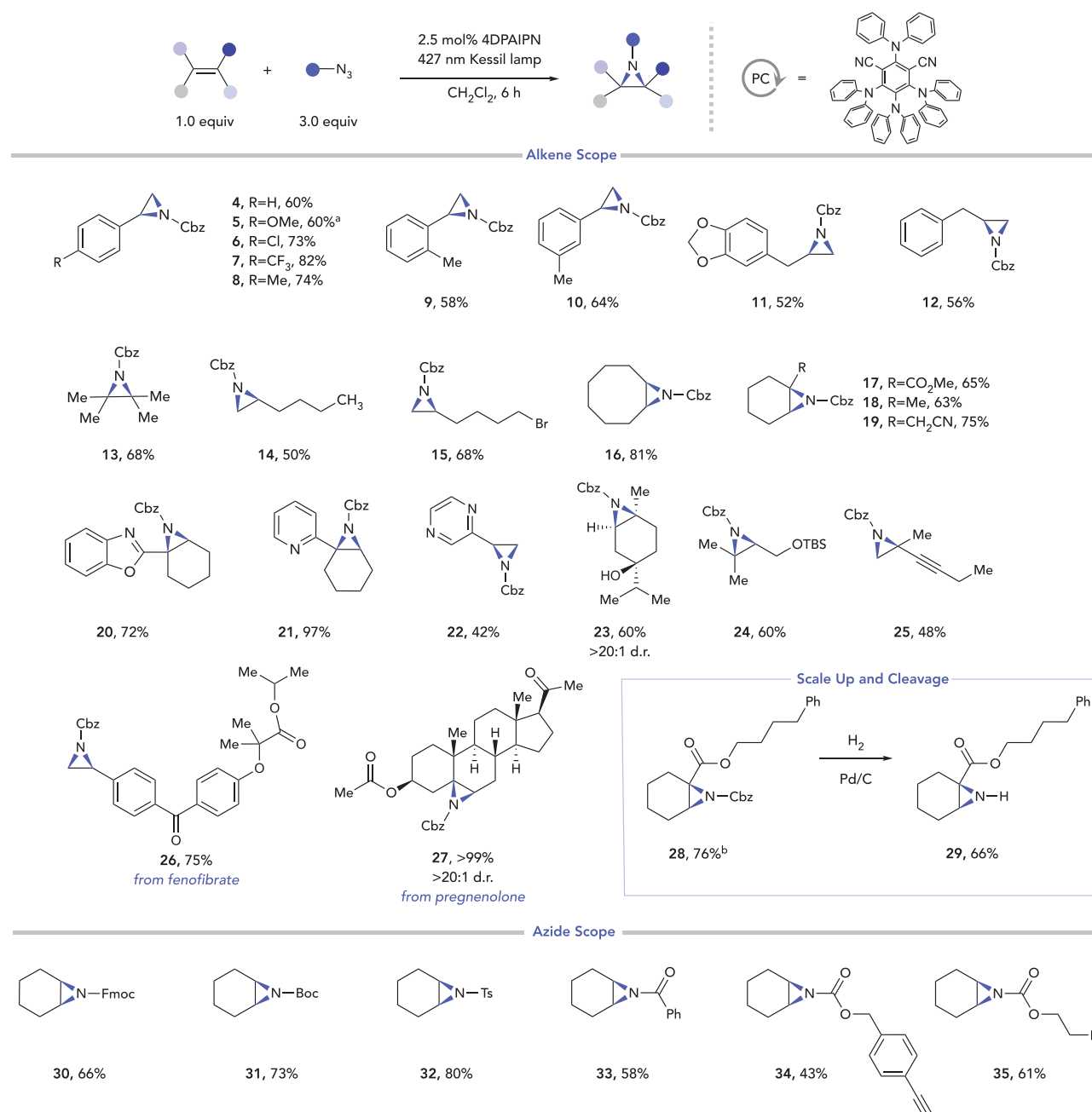
In the past few years, organic chromophores exhibiting thermally activated delayed fluorescence (TADF) have become increasingly recognized as useful photocatalysts that are readily synthesized and span a wide range of photophysical properties.<sup>15,16</sup> Interestingly, while most of the TADF photocatalysts considered here did not result in an improvement in yield (entries 4–6), 4DPAIPN (3g) proved to be remarkably effective in this reaction, providing *N*-Cbz-protected aziridine 2 in 81% yield after 2 h of irradiation (Table 1; entry 7). Control experiments confirmed that both the photocatalyst and light are required for the reaction to occur; in the absence of either, Cbz azide is not consumed (Table 1; entries 8 and 9).

Figure 2 summarizes experiments probing the scope of alkenes that are successfully aziridinated under these optimized conditions, which proved to be quite broad. A range of electronically and sterically varied styrenes undergo aziridination in high yields (4–10). Allylarenes also readily undergo aziridination (11–12), with no observable formation of products resulting from competitive C–H amination of the

**Table 1. Reaction Optimization<sup>a</sup>**

entry	photocatalyst	1	2.5 mol% PC 427 nm Kessil lamp CH <sub>2</sub> Cl <sub>2</sub> , 2 h	2	<i>E</i> <sub>T</sub> (kcal/mol)	<i>E</i> <sub>1/2</sub> (PC <sup>•+</sup> /PC <sup>*</sup> ) (V vs SCE)	<i>τ</i> (μs)	yield
1	$[\text{Ir}(\text{ppy})_2(\text{dtbbpy})]\text{PF}_6$ (3a)				51	−0.96	0.56	32%
2	<i>fac</i> - $[\text{Ir}(\text{ppy})_3$ (3b)				63	−1.73	1.3	34%
3	$[\text{Ir}(\text{dFCF}_3\text{ppy})_2(\text{dtbbpy})]\text{PF}_6$ (3c)				61	−0.89	2.3	4%
4	4CzIPN (3d)				62	−1.24	1.5	7%
5	5CzBN (3e)				65	−1.42	7.8	25%
6	4CICzIPN (3f)				62	−0.63	1.4	2%
7	4DPAIPN (3g)				53	−1.28	104	81%
8 <sup>b</sup>	4DPAIPN (3g)				53	−1.28	104	0%
9	no catalyst				—	—	—	0%

<sup>a</sup>Reactions conducted using 1.0 equiv of cyclohexene and 3.0 equiv of 1. Yields determined by <sup>1</sup>H NMR analysis against 1-methylnaphthalene as an internal standard. Irradiation was conducted using a 427 nm Kessil lamp unless otherwise noted. <sup>b</sup>Reaction conducted in the dark.



**Figure 2.** Substrate scope. Aziridinations were performed on 0.40 mmol scale using 1.0 equiv alkene, 3.0 equiv azide, 2.5 mol % 4DPAIPN, and  $\text{CH}_2\text{Cl}_2$  unless otherwise noted. Reactions were irradiated in a water bath for 6 h using a 427 nm Kessil lamp. <sup>a</sup>Yield determined by  $^1\text{H}$ NMR using dibromomethane as internal standard. <sup>b</sup>Reaction conducted on 1 mmol scale.

highly activated central methylene unit.<sup>17</sup> Simple acyclic (13–15) and cyclic aliphatic alkenes (16–19) are also readily aziridinated, as is an electron-deficient enoate ester (17). Substrates bearing a variety of Lewis basic heterocycles including benzoxazole (20), pyridine (21), and pyrazine (22) are well tolerated; these pharmaceutically valuable motifs are often incompatible with transition metal catalyzed nitrene transfer methods due to competitive coordination to the metal, but they did not present problems for this organophotocatalytic method. The functional group compatibility is also broad, as substrates featuring free alcohols (23), silyl ethers (24), and alkynes (25) are aziridinated in good yields. When applied to more complex medicinally relevant alkenes including a

fenofibrate derivative (26) and pregnenolone acetate (27), the aziridination proceeded smoothly. The reaction can be conducted on a 1.0 mmol scale (28) with no alteration of the reaction conditions, and the aziridine can be isolated in yields comparable to smaller scales (76%). Importantly, this material is easily deprotected under standard hydrogenative conditions for Cbz cleavage to reveal the free N–H aziridine.

An important goal of this study was to expand the range of nitrene precursors that could be used for photocatalytic aziridination reactions. In this vein, we have found that the conditions optimized for aziridination using Cbz azide translate smoothly to other carbamoyl azides, and aziridines featuring N-Fmoc (30) and N-Boc (31) groups are isolated in

good yields. Tosyl azide was also sensitized to afford *N*-Ts aziridine (32) in good yield, showcasing the ability to prepare the same class of aziridines accessible using the Koenigs and Codée methods. Aziridination using benzoyl azide was also high-yielding (33), suggesting that the rate of aziridination was faster than Curtius rearrangement, a common decomposition pathway available for acyl nitrenes.<sup>18</sup> These results inspired us to investigate other acyl azides featuring moieties that might also react with the photogenerated nitrene at competitive rates. A carbamoyl azide featuring an alkyne group participated in aziridination in 43% yield (34), and no products arising from competitive reaction with the alkyne were observed. Interestingly, although photogenerated nitrenes have been invoked in intramolecular C–H insertion reactions, aziridine 35 could be synthesized in good yields without evidence for the formation of an oxazolidone arising from insertion into the benzylic C–H bond.<sup>19,20</sup>

Singlet nitrenes, triplet nitrenes, and nitrene radical anions have each been invoked as intermediates in previously reported photochemical aziridination reactions.<sup>7–11</sup> To distinguish among these possibilities, we utilized a combination of synthetic and computational methods (Figure 3). First,

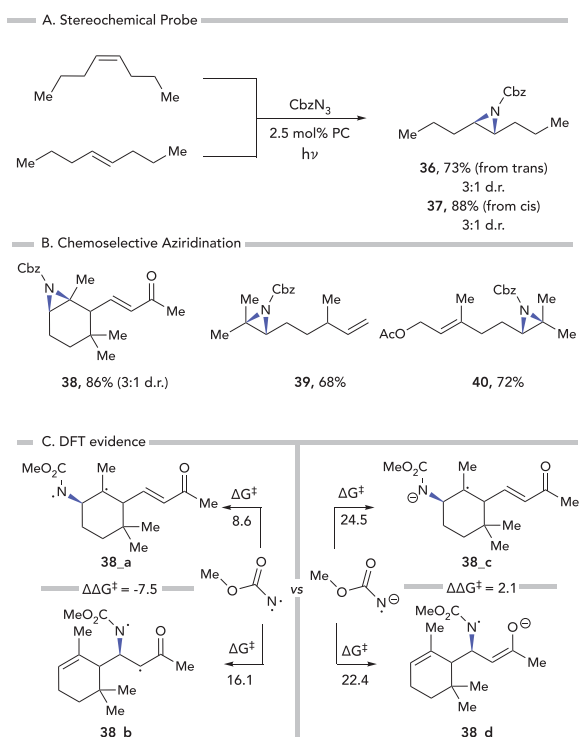


**Figure 3.** Studies supporting a triplet nitrene reactive intermediate. (A) Stereochemical probe; (B) Chemoselective aziridination at electron rich olefins; (C) DFT computed activation barriers for aziridination of 38 by triplet nitrene vs nitrene radical anion, performed at M06-2X-D3/def2-TZVPP(SMD)//M06-2X-D3/6-31+G(d,p)(SMD).

subjecting stereochemically well-defined *cis* and *trans* 4-octene to the optimized conditions for aziridination gave identical 3:1 mixtures of *trans* and *cis* diastereomers (36, 37). The stereoconvergency of the reaction is inconsistent with the expected reactivity of a singlet nitrene intermediate, as these reactions are typically concerted and stereospecific (Figure 3A).<sup>21</sup> To distinguish between the possibility of a triplet

nitrene or nitrene radical anion intermediate, we examined the chemoselectivity of the reaction (Figure 3B). Aziridination of  $\alpha$ -ionone resulted in exclusive reaction of the more electron-rich trisubstituted alkene (38), with no observable products arising from competitive aziridination of the electron-deficient enone functionality. This result appears more consistent with the reaction of an electrophilic triplet nitrene intermediate than a nitrene radical anion, which one would expect to have more nucleophilic character. Indeed, when the activation barriers for aziridination by both reactive intermediates were examined by DFT calculations, the experimentally observed selectivity is consistent only with the triplet nitrene (Figure 3C). Computed transition structures (TSs) at the M06-2X-D3/def2-TZVPP-(SMD)//M06-2X-D3/6-31+G(d,p)(SMD) level of theory<sup>22</sup> for  $\alpha$ -ionone (38) show that the triplet nitrene favors reaction at the more electron-rich alkene by 7.5 kcal/mol, whereas the nitrene radical anion favors reaction at the electron-deficient alkene by 2.1 kcal/mol. The exceptionally large computed selectivity of 7.5 kcal/mol suggests that triplet nitrenes may be able to differentiate between alkenes with less pronounced electronic differences. Indeed, further competition experiments reveal that the aziridination reaction exhibits a marked preference for electron-rich alkenes. The reaction of Cbz azide with citronellene results in exclusive aziridination of the trisubstituted alkene over the terminal alkene in 68% yield (39). A similar experiment using geraniol acetate results in 72% yield of aziridination of the trisubstituted alkene distal to the inductively electron-withdrawing acetoxy group (40), along with 16% of the doubly aziridinated product. However, no products arising from exclusive aziridination of the alkene proximal to the acetoxy group were observed.

The superior reactivity of 4DPAIPN among the photocatalysts screened was a valuable but surprising observation. In order to draw inferences about the mechanisms of photocatalytic reactions, it is common practice to examine the yield of a photoreaction as a function of selected photophysical properties.<sup>23</sup> In this study, however, both the triplet-state energy and excited-state reduction potential reported for 4DPAIPN are intermediate among those of the photocatalysts screened (Table 1). The question then becomes why this specific photocatalyst works uniquely well, and for this we turned to photophysical investigations.

These studies were initiated with transient absorption (TA) interrogation of 4DPAIPN in the absence of substrate. TA spectra were collected after pulsed ( $\sim$ 5 ns fwhm) excitation at 470 nm ( $S_1 \leftarrow S_0$  transition, Figure 4A) of 4DPAIPN in acetonitrile, which is the solvent used for all our spectroscopic studies.<sup>24</sup> At all delay times, we observe a ground-state bleach (GSB) juxtaposed to the blue of broad excited state absorption spanning to 600 nm and beyond. The bleach corresponds to loss of the higher energy transition ( $S_2 \leftarrow S_0$  peaked at 390 nm) shown in the absorption spectrum in the lower panel of Figure 4A. The ESA presents as two peaks, but this appears to be a manifestation of bleaching of the lower energy ( $S_1 \leftarrow S_0$ ) transition (peaked at 470 nm) superposed upon the ESA. These spectra decay with time without apparent spectral shifting; decay traces focusing on both the GSB (at 390 nm) and ESA (at 430 nm) are found to decay monoexponentially with an average lifetime of 98  $\mu$ s (see Figure 4B). This corresponds to the observed lifetime of the triplet excited state of 4DPAIPN. Since this photocatalyst is known for its thermally activated delayed fluorescence properties, we were also able to measure the triplet lifetime independently using

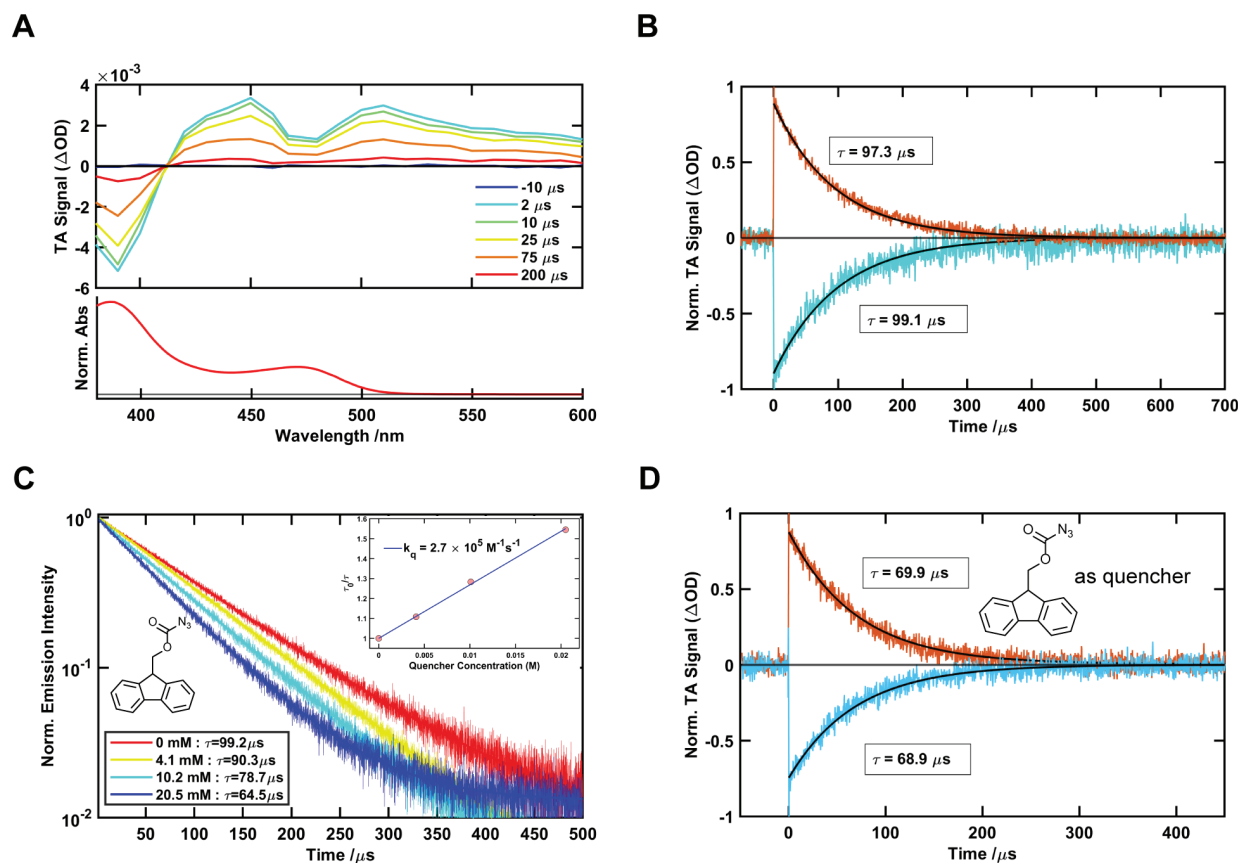


**Figure 4.** Photophysical investigation into excited state reactivity between 4DPAIPN and Fmoc-azide in acetonitrile. (A) Transient absorption (TA) spectra of 4DPAIPN collected by exciting the sample at 470 nm. The time delay between pump and probe for the plotted spectral slices are denoted in the legend. The normalized ground state absorption spectrum of 4DPAIPN is shown for reference. (B) Normalized decay traces corresponding to both ground-state bleach (GSB) at 390 nm and excited state absorption (ESA) at 430 nm features of photoexcited 4DPAIPN without any quenchers. (C) Time-resolved emission spectroscopy monitoring the delayed fluorescence lifetime of 4DPAIPN\* in the presence of varying concentrations of Fmoc-azidoformate. The quencher concentrations and the measured lifetime (obtained from a monoexponential fit) are denoted in the legend. The inset shows a Stern–Volmer plot obtained with this data set. (D) TA experiment monitoring the GSB and ESA kinetic traces of 4DPAIPN\* in the presence of 19.5 mM Fmoc-azide. The data are well-modeled with a monoexponential fit and results in 68.9 and 69.9  $\mu$ s lifetimes for GSB and ESA traces, respectively.

time-resolved emission spectroscopy focusing on features in the fluorescence spectrum of the  $S_1$ . The measured delayed fluorescence lifetime ( $\tau_{DF}$ ) of 99  $\mu$ s matches closely with the value of 98  $\mu$ s obtained via TA. A prompt fluorescence lifetime ( $\tau_{PF}$ ) of 3.7 ns is also evident for this photocatalyst using a shorter time window in time-correlated single photon counting (TCSPC) experiments. The quantity  $\tau_{PF}$  for TADF systems is representative of their  $S_1$  lifetimes.

Having characterized the unquenched triplet lifetime and spectrum, we then monitored the impact of varying concentrations of Fmoc azide acting as a potential quencher. First, time-resolved emission spectroscopy was employed, and as shown in Figure 4C,  $\tau_{DF}$  was indeed found to diminish as the quencher concentration is increased. A plot of quencher concentration versus  $\tau_0/\tau$  ( $\tau_0$  and  $\tau$  are the unquenched and quenched lifetimes respectively) is analyzed to determine a second-order quenching constant of  $k_q = 2.7 \times 10^5 \text{ M}^{-1} \text{ s}^{-1}$  (Figure 4C inset). While quenching is indeed evident, this  $k_q$  is much lower than values obtained in processes rate-limited by diffusion ( $10^9$ – $10^{10} \text{ M}^{-1} \text{ s}^{-1}$ ). Considering that in 4DPAIPN, the singlet ( $S_1$ ) and triplet ( $T_1$ ) excited states store similar amounts of energy, it could be contended that quenching would be observable from either of these excited states.

However, given the short  $S_1$  lifetime (3.7 ns, *vide supra*), a bimolecular quenching rate of  $\sim 10^5 \text{ M}^{-1} \text{ s}^{-1}$  precludes the singlet state from being active under reaction conditions where the azide concentration is only 1.2 M. For comparison, with  $k_q$  of  $10^5 \text{ M}^{-1} \text{ s}^{-1}$  and a substrate concentration of 1.2 M, the quenching process would be only 0.1% efficient with an excited-state lifetime of 10 ns. This is inconsistent with the experimentally determined reaction quantum yield of  $\Phi = 0.78$ .

Second, TA experiments were repeated in the presence of 19.5 mM Fmoc azide (see Figure S5 for the spectral slices). A quenched triplet lifetime of 69  $\mu$ s, consistent with  $k_q = 2.7 \times 10^5 \text{ M}^{-1} \text{ s}^{-1}$ , was observed from both the GSB and ESA kinetic traces (Figure 4D). The decay profiles are cleanly modeled with monoexponential functions with no long-lived or time-independent components that might manifest as an offset, if present. These observations imply ground-state recovery of 4DPAIPN during quenching. This in turn is consistent with an energy transfer mechanism. By contrast, electron transfer (ET) would generate the radical cation of 4DPAIPN and in the limit that back-ET is not rapid, this would (a) prevent recovery of the GSB in a monoexponential fashion, and (b) result in new absorptive features around 425 and 515 nm in the TA spectra (see Figure S7 for the absorption spectrum of 4DPAIPN $^{*+}$ ).

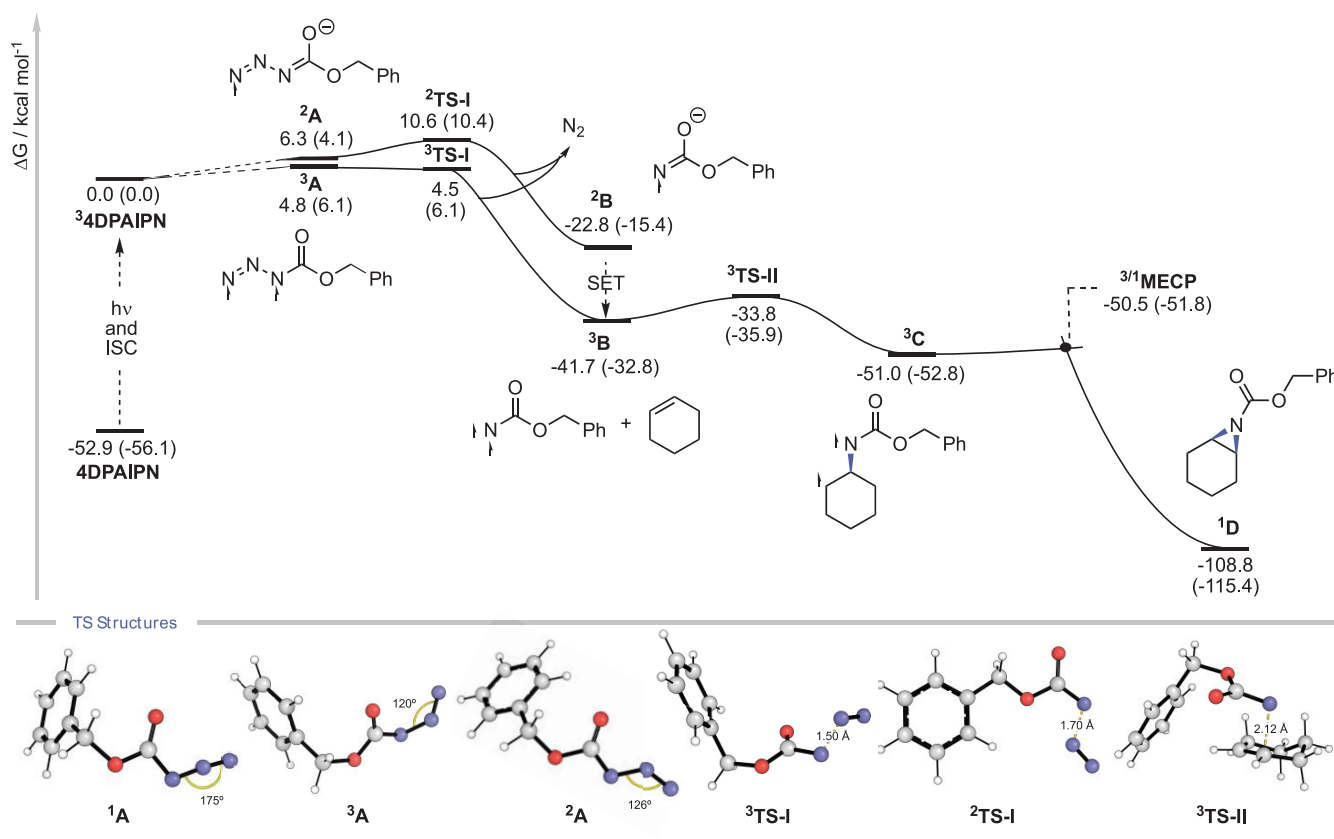


**Figure 5.** Computed potential energy surface (PES) in kcal/mol for the aziridination of cyclohexene using  $\text{N}_3\text{Cbz}$  at the M06-2X-D3/def2-TZVPP(SMD)//M06-2X-D3/6-31+G(d,p)(SMD) level of theory; electronic energies ( $E$ ) are shown in parentheses; Gibbs energy of the MECP was estimated using projected frequencies.

While we favor assignment to energy transfer as the simplest explanation of our observations, these measurements do not inherently rule out the possibility of an ET-mediated quenching mechanism if the rate of BET is significantly faster than the forward process.<sup>20</sup>

As the likely energy transfer reactivity stems from the triplet excited state, a Dexter mechanism would be expected. Here, the  $^3\text{4DPAIPN}^*$  first generates triplet azide while returning to its ground state. The sensitized triplet azide is then expected to rapidly lose dinitrogen ( $\text{N}_2$ ) generating triplet nitrene and unreactive  $\text{N}_2$ . Since the nitrene in this case is not expected to have visible  $\text{T}_n \leftarrow \text{T}_0$  transitions, the lack of new absorptive features in measured TA spectra is justified.

We return to **Table 1** that considered aziridination yields over a range of photocatalysts. If we assume that each operates via the same Dexter energy transfer mechanism, several observations emerge that can inform photocatalyst design. First, a comparison of entries 1 and 4 highlights favorable properties of iridium-based photocatalyst **3a** over carbazole-based organic photocatalyst **4CzIPN** (**3d**). Whereas **3a** possesses a lower  $E_T$  (51 kcal/mol) and a shorter  $\tau$  (0.56  $\mu\text{s}$ ) compared to **3d** ( $E_T = 62$  kcal/mol,  $\tau = 1.5$   $\mu\text{s}$ ), the higher product yield from **3a** suggests higher efficiency in the energy transfer process when appropriate collisions do occur. This could be related to the nature of the  $\text{T}_1$  frontier molecular orbitals, which are very different between these two families of photocatalysts. Entries 1 and 3, while both Ir-based photocatalysts, support this idea. Even though **3c** should be superior to **3a** based on an enhanced  $E_T$  (61 kcal/mol versus

51 kcal/mol) and lengthened  $\tau$  (2.3  $\mu\text{s}$  versus 0.56  $\mu\text{s}$ ), its aziridination yield is poor, consistent with diminished orbital overlap between the triplet photocatalyst and the azide resulting from the bulkier ligands in **3c**. While energy transfer efficiency per collision may be suboptimal in the organic photocatalysts of **Table 1**, triplet lifetime can assist. This is first seen in comparisons among entries 4, 5, and 6 where each carbazole-based photocatalyst **3d**, **3e**, and **3f** has a similar  $E_T$ . Despite these energetic similarities, the reaction yield is largest for **5CzBN** (**3e**) where the lifetime of 7.8  $\mu\text{s}$  is more than a factor of 5 longer than what is available to **4CzIPN** (**3d**) or **4ClCzIPN** (**3f**). Continuing in this vein offers a satisfying rationale for the superior performance of **4DPAIPN** (**3g**). Here the inclusion of diphenylamino substituents over the more rigid carbazoles (a direct comparison between the structurally similar **4DPAIPN** (**3g**) and **4CzIPN** (**3d**) is most straightforward) leads to a marked lifetime enhancement (99  $\mu\text{s}$  versus 1.5  $\mu\text{s}$ ) and with it a dramatic enhancement of reaction yield (81% versus 7%). We presume that the lifetime enhancement in **4DPAIPN** is a consequence of a larger  $S_1 - T_1$  energy gap for that photocatalyst (thus slowing down reverse intersystem crossing) and that in turn is made possible by the more flexible diphenylamino substituents, which can accommodate photocatalyst geometries that enhance exchange interactions between the unpaired electrons of the  $S_1$  and the  $T_1$  states.

The M06-2X-D3/def2-TZVPP(SMD)//M06-2X-D3/6-31+G(d,p) computed potential energy surface (PES) for the aziridination of cyclohexene by Cbz azide is shown in **Figure 5**. Azide **1** has a calculated adiabatic triplet energy of 57.7 kcal/

mol; the 4DPAIPN photocatalyst has a calculated adiabatic triplet energy of 52.9 kcal/mol, closely matching the experimentally determined triplet energy of 52.8 kcal/mol. The computed thermochemistry for electron transfer vs energy transfer to azidoformate is similar, with both pathways being endergonic ( $\Delta G = 4.8$  vs 6.3 kcal/mol, respectively). Triplet sensitization is favored at this level of theory by 2.3 kcal/mol. In  $^3\text{A}$ , azide bending out of the amide plane occurs to place the two unpaired electrons in orthogonal orbitals on the two terminal N atoms; in contrast,  $^2\text{A}^{\bullet-}$  adopts a planar-bent distonic structure in which most of the negative charge is localized on O, with the spin on the terminal N.

Loss of  $\text{N}_2$  from  $^3\text{A}$  is close to being energetically barrierless, via  $^3\text{TS-I}$ , forming triplet nitrene  $^3\text{B}$  in highly exergonic fashion. For the electron-transfer pathway, loss of  $\text{N}_2$  from  $^2\text{A}$  is also relatively facile, via  $^2\text{TS-I}^{\bullet-}$  ( $\Delta G^{\ddagger} = 4.3$  kcal/mol), forming  $^2\text{B}$ .<sup>25</sup> Thermodynamically favorable BET from this species to the oxidized photocatalyst would then lead to triplet nitrene  $^3\text{B}$ . Once the triplet nitrene is generated, radical addition to cyclohexene via  $^3\text{TS-II}$  has a readily accessible barrier ( $\Delta G^{\ddagger} = 7.9$  kcal/mol), leading to the formation of the triplet 1,3-diradical  $^3\text{C}$ . A low-lying minimum energy crossing point (MECP) was identified in the vicinity of the intermediate  $^3\text{C}$ , which closely resembles the geometry of the triplet structure. This is indicative of a facile intersystem crossing (ISC) process from  $\text{T}_1$  to  $\text{S}_0$ , upon which the formal singlet diradicaloid species undergoes barrierless recombination to form aziridine **D** in highly exergonic and irreversible fashion.

## CONCLUSIONS

4DPAIPN is an exceptional photocatalyst for the aziridination of alkenes, and its superior reactivity enables the use of a range of azides as nitrene precursors. This improved method for photocatalytic aziridination has a broad substrate scope and tolerates Lewis basic functionalities that would challenge transition metal catalyzed methods. A combination of computational, spectroscopic, and synthetic experiments supports the intermediacy of a triplet nitrene that exhibits exquisite selectivity for reaction with more electron-rich alkenes in compounds with multiple possible sites of reaction. Both time-resolved emission and TA spectroscopy demonstrate quenching of 4DPAIPN triplet lifetime through reaction with azides such as Fmoc-N<sub>3</sub>. TA experiments indicate full recovery of ground-state bleach features of the photocatalyst during such reactivity, an observation that is consistent with Dexter triplet energy transfer to the azide. The second order quenching rate of  $2.7 \times 10^5 \text{ M}^{-1} \text{ s}^{-1}$  determined with Fmoc-azide, is much slower than the diffusion limit. Therein, the long triplet lifetime of 4DPAIPN provides a rationale for why it outperforms related TADF photocatalysts.

## ASSOCIATED CONTENT

### Supporting Information

The Supporting Information is available free of charge at <https://pubs.acs.org/doi/10.1021/acscatal.4c03167>.

Experimental procedures, characterization data for new compounds, absorption and emission spectra, electrochemical data, NMR spectra, full computational details, absolute energies, and Cartesian coordinates of all stationary points ([PDF](#))

## AUTHOR INFORMATION

### Corresponding Authors

Niels H. Damrauer — Department of Chemistry and Renewable and Sustainable Energy Institute (RASEI), University of Colorado Boulder, Boulder, Colorado 80309, United States; [orcid.org/0000-0001-8337-9375](https://orcid.org/0000-0001-8337-9375); Email: [niels.damrauer@colorado.edu](mailto:niels.damrauer@colorado.edu)

Robert S. Paton — Department of Chemistry, Colorado State University, Fort Collins, Colorado 80523, United States; [orcid.org/0000-0002-0104-4166](https://orcid.org/0000-0002-0104-4166); Email: [robert.paton@colostate.edu](mailto:robert.paton@colostate.edu)

Tehshik P. Yoon — Department of Chemistry, University of Wisconsin—Madison, Madison, Wisconsin 53706, United States; [orcid.org/0000-0002-3934-4973](https://orcid.org/0000-0002-3934-4973); Email: [tyoon@chem.wisc.edu](mailto:tyoon@chem.wisc.edu)

### Authors

Alana Rose Meyer — Department of Chemistry, University of Wisconsin—Madison, Madison, Wisconsin 53706, United States; [orcid.org/0009-0004-8475-3778](https://orcid.org/0009-0004-8475-3778)

Mihai V. Popescu — Department of Chemistry, Colorado State University, Fort Collins, Colorado 80523, United States; [orcid.org/0000-0001-8565-7201](https://orcid.org/0000-0001-8565-7201)

Arindam Sau — Department of Chemistry, University of Colorado Boulder, Boulder, Colorado 80309, United States; [orcid.org/0009-0002-2097-4673](https://orcid.org/0009-0002-2097-4673)

Complete contact information is available at: <https://pubs.acs.org/10.1021/acscatal.4c03167>

### Notes

The authors declare no competing financial interest.

## ACKNOWLEDGMENTS

This research was supported by the National Science Foundation (NSF) Under the CCI Center for Sustainable Photoredox Catalysis (CHE-2318141). A.R.M. is grateful to the NSF for a graduate research fellowship. NMR and MS facilities at UW—Madison are funded by the NIH (S10OD012245), NSF (CHE-9304546), and a generous gift from the Paul J. and Margaret M. Bender Fund. R.S.P. acknowledges the Alpine high performance computing resource, jointly funded by the University of Colorado Boulder, the University of Colorado Anschutz, and Colorado State University, and ACCESS through allocation TG CHE180056.

## REFERENCES

- (1) Dequina, H. J.; Jones, C. L.; Schomaker, J. M. Recent Updates and Future Perspectives in Aziridine Synthesis and Reactivity. *Chem.* **2023**, *9*, 1658–1701.
- (2) Dank, C.; Ielo, L. Recent Advances in the Accessibility, Synthetic Utility, and Biological Applications of Aziridines. *Org. Biomol. Chem.* **2023**, *21*, 4553–4573.
- (3) Lowden, P. A. S. Aziridine Natural Products—Discovery, Biological Activity and Biosynthesis. In *Aziridines and Epoxides in Organic Synthesis*; Yudin, A. K., Ed. Wiley, 2006; pp 399–442.
- (4) Dembitsky, V. M.; Terentev, A. O.; Levitsky, D. O. *Aziridine Alkaloids: Origin, Chemistry and Activity*. In *Natural Products*; Springer: Berlin, Heidelberg, 2013; pp 977–1006.
- (5) Bera, M.; Lee, D. S.; Cho, E. J. Advances in N-Centered Intermediates by Energy Transfer Photocatalysis. *Trends Chem.* **2021**, *3*, 877–891.
- (6) (a) Mitchell, J. K.; Hussain, W. A.; Bansode, A. H.; O'Connor, R. M.; Parasram, M. Aziridination via Nitrogen-Atom Transfer to Olefins

from Photoexcited Azoxy-Triazenes. *J. Am. Chem. Soc.* **2024**, *146*, 9499–9505. (b) Kobayashi, Y.; Masakado, S.; Takemoto, Y. Photoactivated *N*-Acyliminoiodinanes Applied to Amination: An *ortho*-Methoxymethyl Group Stabilizes Reactive Precursors. *Angew. Chem., Int. Ed.* **2018**, *57*, 693–697.

(7) Scholz, S. O.; Farney, E. P.; Kim, S.; Bates, D. M.; Yoon, T. P. Spin-Selective Generation of Triplet Nitrenes: Olefin Aziridination through Visible-Light Photosensitization of Azidoformates. *Angew. Chem., Int. Ed.* **2016**, *55*, 2239–2242.

(8) Lwowski, W.; Mattingly, T. W., Jr The Decomposition of Ethyl Azidoformate in Cyclohexene and in Cyclohexane. *J. Am. Chem. Soc.* **1965**, *87*, 1947–1958.

(9) Lwowski, W. Nitrenes and the Decomposition of Carbonylazides. *Angew. Chem., Int. Ed. Engl.* **1967**, *6*, 897–906.

(10) Guo, Y.; Pei, C.; Koenigs, R. M. A Combined Experimental and Theoretical Study on the Reactivity of Nitrenes and Nitrene Radical Anions. *Nat. Commun.* **2022**, *13*, 86.

(11) Guo, Y.; Pei, C.; Jana, S.; Koenigs, R. M. Synthesis of Trifluoromethylated Aziridines via Photocatalytic Amination Reaction. *ACS Catal.* **2021**, *11*, 337–342.

(12) For an intriguing Pauson–Khand-type reaction involving direct photoexcitation of iminoiodinanes, see: Li, F.; Zhu, W. F.; Empel, C.; Datsenko, O.; Kumar, A.; Xu, Y.; Ehrler, J. H. M.; Atodiresei, I.; Knapp, S.; Mykhailiuk, P. K.; Proschak, E.; Koenigs, R. M. Photosensitization enables Pauson–Khand-type reactions with nitrenes. *Science* **2024**, *383*, 498–503.

(13) Dam, D.; Lagerweij, N. R.; Janmaat, K. M.; Kok, K.; Bouwman, E.; Codée, J. D. C. Organic Dye-Sensitized Nitrene Generation: Intermolecular Aziridination of Unactivated Alkenes. *J. Org. Chem.* **2024**, *89*, 3251–3258.

(14) Ju, M.; Schomaker, J. M. Nitrene Transfer Catalysts for Enantioselective C–N Bond Formation. *Nat. Rev. Chem.* **2021**, *5*, 580–594.

(15) Bryden, M. A.; Zysman-Colman, E. Organic Thermally Activated Delayed Fluorescence (TADF) Compounds Used in Photocatalysis. *Chem. Soc. Rev.* **2021**, *50*, 7587–7680.

(16) Values for the triplet excited-state energies, excited-state reduction potentials, and excited-state lifetimes for Table 1, entries 1–6 are from ref 15. Values for entries 7 and 8 are from: Kwon, Y.; Lee, J.; Noh, Y.; Kim, D.; Lee, Y.; Yu, C.; Roldao, J. C.; Feng, S.; Gierschner, J.; Wannemacher, R.; Kwon, M. S. Formation and Degradation of Strongly Reducing Cyanoarene-Based Radical Anions towards Efficient Radical Anion-Mediated Photoredox Catalysis. *Nat. Commun.* **2023**, *14*, 92.

(17) Li, H.-H.; Chen, X.; Kramer, S. Recent developments for intermolecular enantioselective amination of non-acidic C(sp<sup>3</sup>)–H bonds. *Chem. Sci.* **2023**, *14*, 13278–13289.

(18) Liu, J.; Mandel, S.; Hadad, C. M.; Platz, M. S. A Comparison of Acetyl- and Methoxycarbonylnitrenes by Computational Methods and a Laser Flash Photolysis Study of Benzoylnitrene. *J. Org. Chem.* **2004**, *69*, 8583–8593.

(19) Jung, H.; Keum, H.; Kweon, J.; Chang, S. Tuning Triplet Energy Transfer of Hydroxamates as the Nitrene Precursor for Intramolecular C(sp<sup>3</sup>)–H Amidation. *J. Am. Chem. Soc.* **2020**, *142*, 5811–5818.

(20) Bouayad-Gervais, S.; Nielsen, C. D.-T.; Turksoy, A.; Sperger, T.; Deckers, K.; Schoenebeck, F. Access to Cyclic *N*-Trifluoromethyl Ureas through Photocatalytic Activation of Carbamoyl Azides. *J. Am. Chem. Soc.* **2022**, *144*, 6100–6106.

(21) Lwowski, W.; McConaghay, J. S., Jr Carbethoxynitrene. Control of the Stereospecificity of an Addition to Olefins. *J. Am. Chem. Soc.* **1965**, *87*, 5490–5491.

(22) Computations used the Gaussian 16 rev. C.01. For full computational details and references please see Supporting Information.

(23) For a review, see: Cahoon, S. B.; Yoon, T. P., *Photochemistry and Radical Generation: Approaches in Mechanism Elucidation*. In *Science of Synthesis: Free Radicals: Fundamentals and Applications* in Organic Synthesis, Fensterbank, L.; Ollivier, C., Eds.; Thieme: Stuttgart, 2021; Vol. 1, pp 159–205.

(24) Acetonitrile was chosen as a solvent because of its ability to stabilize charged intermediates that would be produced following an electron transfer.

(25) The half-life of <sup>2</sup>A would be ~0.15 ns according to transition state theory if this pathway is operative. This suggests that the rebound mechanism described in ref 20 cannot be ruled out at this time.